

Supporting Information
for
**“Proteome-wide Discovery and Characterizations of Nucleotide-
binding Proteins with Affinity-labeled Chemical Probes”**

Anal. Chem. 2013, Vol. 85 (ac-2012-03383c)

Yongsheng Xiao, Lei Guo, Xinning Jiang, Yinsheng Wang*

Department of Chemistry, University of California, Riverside, CA 92521-0403

*To whom correspondence should be addressed: yinsheng.wang@ucr.edu. Tel.: (951) 827-2700;
Fax: (951) 827-4713.

Supplementary Experimental Details

Preparation of Biotinylated Nucleotide Affinity Probe

The biotinylated nucleotide affinity probes were prepared according to previously published procedures with minor modifications¹. Briefly, probes were synthesized by directly conjugating biotin-LC or desthiobiotin with ATP or GTP. To render nucleotides soluble in organic solvent, the commercially available sodium salt form of nucleotides were first converted to the tributylammonium form by passing the nucleotides through a cation-exchange column packed with Spectra/Gel IE 50×8 resin (40-75 μm) at 4°C once. The tributylammonium form of nucleotide fractions were collected and lyophilized. Biotin-LC (10 mg) or desthiobiotin (6 mg), dissolved in a 1-mL solvent mixture of ice-cold dry CH₂Cl₂ and DMF (4:1, v/v), was mixed with tri-*n*-butylamine (11 μL) and ethyl chloroformate (5 μL). After stirring at 0°C for 5 min, the mixture was stirred at room temperature under argon atmosphere for another 60 min. Tributylammonium form of nucleotides (50 mg), dissolved in a 1.25-mL solution of CH₂Cl₂ and DMF (4:1, v/v), was then added to the above reaction mixture. The reaction was continued at room temperature and under argon atmosphere for 18 hr. The CH₂Cl₂ was then removed by argon purging for 10 min and the remaining 200 μL solution was directly subjected to HPLC purification with a YMC ODS-AQ column (4.8×250 mm, 120 Å in pore size, 5 μm in particle size, Waters). The flow rate was 0.8 mL/min, and a 45-min linear gradient of 0-30% acetonitrile in 50 mM triethylammonium acetate (pH 6.8) was used for the purification. A UV detector was set at 265 nm to monitor the effluents. Appropriate HPLC fractions were pooled, lyophilized, and stored at -80°C. The structures of the products were confirmed by ESI-MS and MS/MS.

SDS-PAGE Separation and In-Gel Digestion

The labeled proteins were denatured by boiling in Laemmli loading buffer for 5 min, and separated by a 12% SDS-PAGE with 4% stacking gel. The gel was stained with Coomassie blue; after destaining, the gel was cut into 8 slices, and the proteins were reduced in-gel with DTT and alkylated with IAM. The proteins were digested in-gel with modified sequencing-grade trypsin overnight, after which peptides were extracted from the gels with 5% acetic acid in H₂O and subsequently with 5% acetic acid in CH₃CN/H₂O (1:1, v/v). The resultant fractions of peptide mixtures were dried and stored at -20°C for further avidin enrichment.

Fractionation of Biotinylated Peptides with SCX Chromatography

Biotinylated peptides were desalted using C18 OMIX tips (Agilent) and subsequently loaded onto SCX TopTips (PolyLC). The bound peptides were sequentially eluted into 9 fractions with increasing KCl concentrations from 0.01 to 0.5 M. The peptides in each fraction were subjected to desalting again using C18 OMIX tips prior to LC-MS/MS analysis.

LC-MS/MS Analysis

LC-MS/MS analysis was performed on an LTQ-Orbitrap Velos mass spectrometer equipped with a nanoelectrospray ionization source (Thermo Fisher Scientific, San Jose, CA). Samples with or without SDS-PAGE and SCX pre-fractionation (procedures shown in the Supporting Information) were automatically loaded from a 48-well microplate autosampler using an EASY-nLC system (Proxeon Biosystems, Odense, Denmark) at 3 μL/min onto a home-made 4 cm trapping column (150 μm i.d.) packed with 5 μm C18 120 Å reversed-phase material (ReproSil-Pur 120 C18-AQ, Dr. Maisch). The trapping column was connected to a 20 cm fused

silica analytical column (PicoTip Emitter, New Objective, 75 μm i.d.) with 3 μm C18 beads (ReproSil-Pur 120 C18-AQ, Dr. Maisch). The peptides were then separated with a 120-min linear gradient of 2-35% acetonitrile in 0.1% formic acid and at a flow rate of 250 nL/min. The LTQ-Orbitrap Velos was operated in data-dependent scan mode. Full-scan mass spectra were acquired in the Orbitrap analyzer with a resolution of 60000 with lock mass option enabled for the ion of m/z 445.120025². Up to 20 most abundant ions found in MS with charge state ≥ 2 were sequentially isolated and sequenced in the linear ion trap with a normalized collision energy of 35, an activation q of 0.25 and an activation time of 10 ms.

Online 2D LC Separation and LC-MS/MS analysis

The fully automated 7-cycle on-line two-dimensional LC-MS/MS was set up as described³. Briefly, the C18 trapping column was replaced with a biphasic precolumn (150 μm i.d.) comprised of a 3.5-cm column packed with 5 μm C18 120 Å reversed-phase material (ReproSil-Pur 120 C18-AQ, Dr. Maisch) and 3.5-cm column packed with Luna 5 μm SCX 100 Å strong cation exchange resin (Phenomenex, Torrance, CA) while all other setups remained the same. Enriched biotinylated peptides were first loaded onto the biphasic precolumn. Ammonium acetate at concentrations of 0, 25, 50, 75, 125, 200 and 500 mM were then sequentially injected using a 48-well autosampler from the sample vial to elute bound peptides from precolumn to analytical column with reversed-phase separation. LC-MS/MS experiments were also performed with a 120-min linear gradient of 2-35% acetonitrile in 0.1% formic acid.

Data Processing and Analysis.

For peptide identification, the raw data acquired were processed with the Maxquant search engine (version 1.2.0.18)⁴ against human IPI protein database version 3.68 which contained 87,062 entries. Initial precursor mass tolerance of 10 ppm and fragment mass deviation of 0.8 Th were set as the search criteria. The maximum number of miss-cleavages for trypsin was set as two per peptide. Cysteine carbamidomethylation was considered as a fixed modification, whereas methionine oxidation and lysine biotinylation (+339.161662 Da) or desthiobiotinylation (+196.121178 Da) were included as variable modifications. The reverse database search option was enabled to filter the search results to satisfy a maximum false discovery rate of 1%.

For SILAC-based comparison experiment, the raw data were converted to mzXML files and DTA files using ReAdW (<http://sourceforge.net/projects/sashimi/files/>) and MzXML2Search (<http://tools.proteomecenter.org/wiki/index.php?title=Software:MzXML2Search>) programs, respectively. Bioworks 3.2 was used for protein identification by searching the DTA files against the human IPI protein database version 3.68 and its reversed complement. Aside from the search parameters described above, lysine (+8 Da) and arginine (+6 Da) mass shifts introduced by heavy isotope labeling were considered as variable modifications. The search results were then filtered with DTASelect⁵ to achieve a peptide false discovery rate of 1%. Census was employed for peptide and protein quantification⁶. Extracted-ion chromatograms were first generated for peptide ions based on their m/z values and peptide intensity ratios were subsequently calculated in Census from peak areas found in each pair of extracted-ion chromatograms.

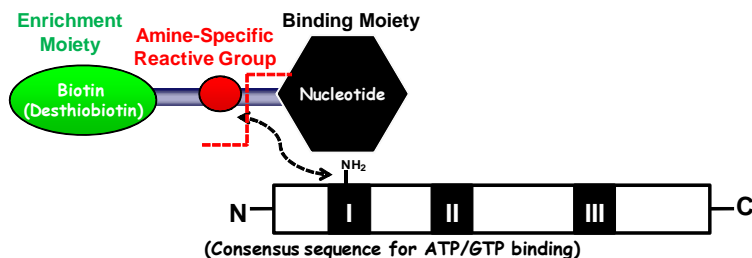
Supplementary Reference

1. Qiu, H.; Wang, Y., Probing adenosine nucleotide-binding proteins with an affinity-labeled nucleotide probe and mass spectrometry. *Anal. Chem.* **2007**, *79* (15), 5547-5556.
2. Olsen, J. V.; de Godoy, L. M. F.; Li, G.; Macek, B.; Mortensen, P.; Pesch, R.; Makarov, A.; Lange, O.; Horning, S.; Mann, M., Parts per Million Mass Accuracy on an Orbitrap Mass Spectrometer via Lock Mass Injection into a C-trap. *Mol. Cell. Proteomics* **2005**, *4* (12), 2010-2021.
3. Taylor, P.; Nielsen, P. A.; Trelle, M. B.; Andersen, M. B.; Vorm, O.; Moran, M. F.; Kislinger, T., Automated 2D peptide separation on a 1D Nano-LC-MS system. *J. Proteome Res.* **2009**, *8* (3), 1610-1616.
4. Cox, J.; Mann, M., MaxQuant enables high peptide identification rates, individualized p.p.b.-range mass accuracies and proteome-wide protein quantification. *Nat Biotech* **2008**, *26* (12), 1367-1372.
5. Tabb, D. L.; McDonald, W. H.; Yates, J. R., DTASelect and Contrast: □ tools for assembling and comparing protein identifications from shotgun proteomics. *J. Proteome Res.* **2002**, *1* (1), 21-26.
6. Park, S. K.; Venable, J. D.; Xu, T.; Yates, J. R., A quantitative analysis software tool for mass spectrometry-based proteomics. *Nat Meth* **2008**, *5* (4), 319-322.

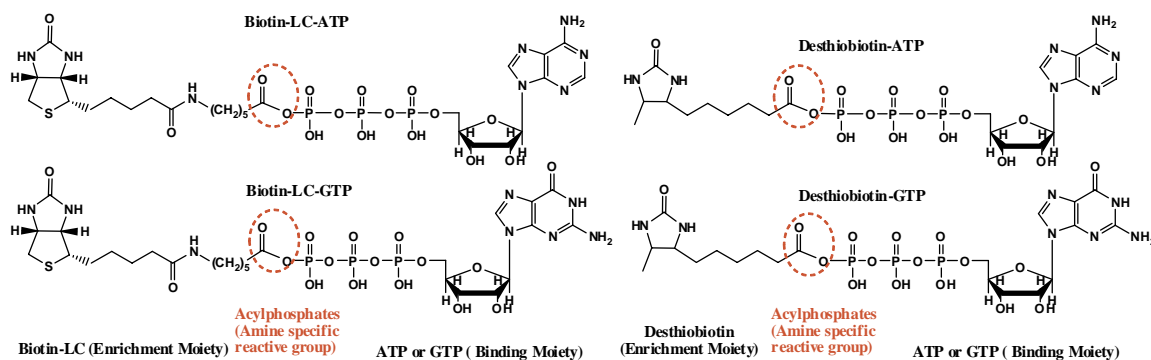
Supplementary Figures

Figure S1. (A) The design of nucleotide-affinity probe. (B) The structures of biotin-based ATP/GTP probes and desthiobiotin-based ATP/GTP probes. (C) The representative HPLC trace for the purification of the crude product of nucleotide-affinity probe. (D) Representative of ESI-MS of purified biotin-based ATP/GTP probes and desthiobiotin-based ATP/GTP probes

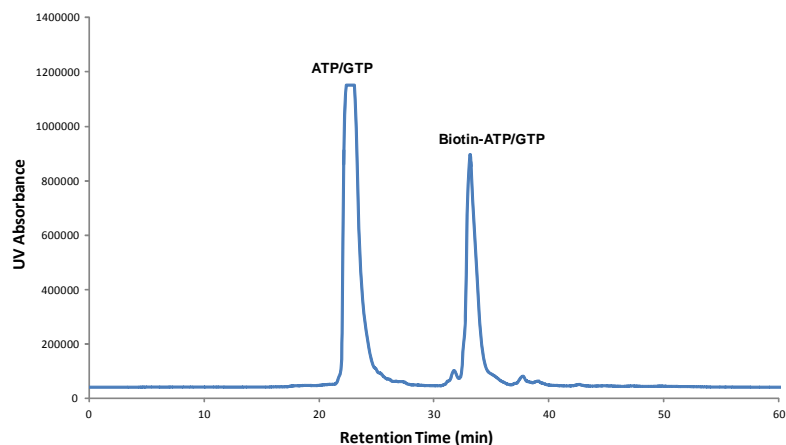
(A)



(B)



(C)



(D)

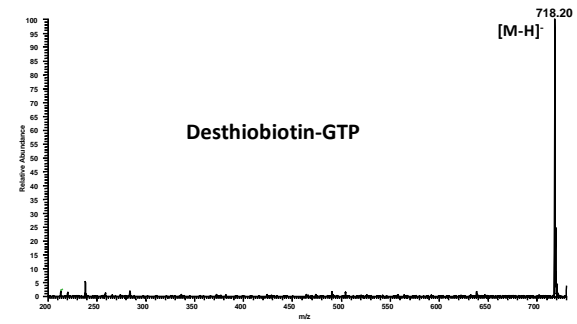
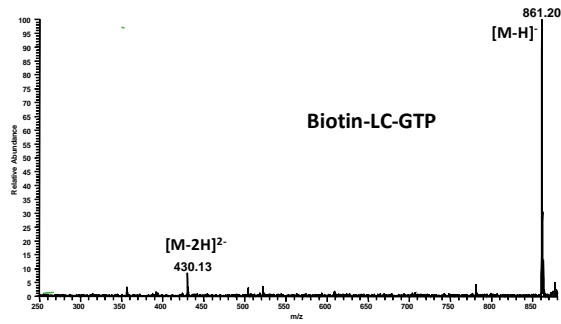
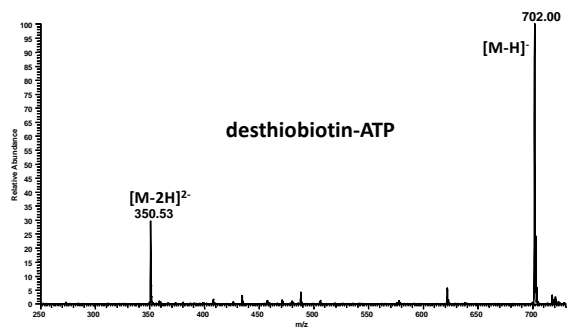
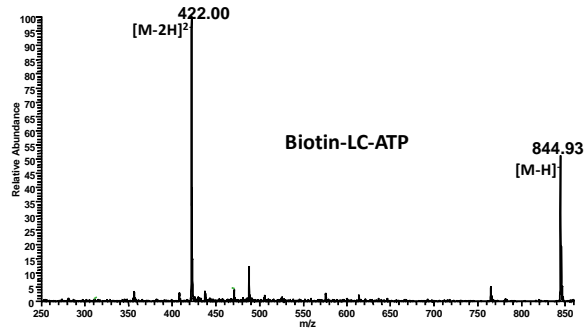


Figure S2. A scheme showing the enrichment and identification of nucleotide-binding proteins from human whole proteome with biotin-based ATP/GTP affinity probe.

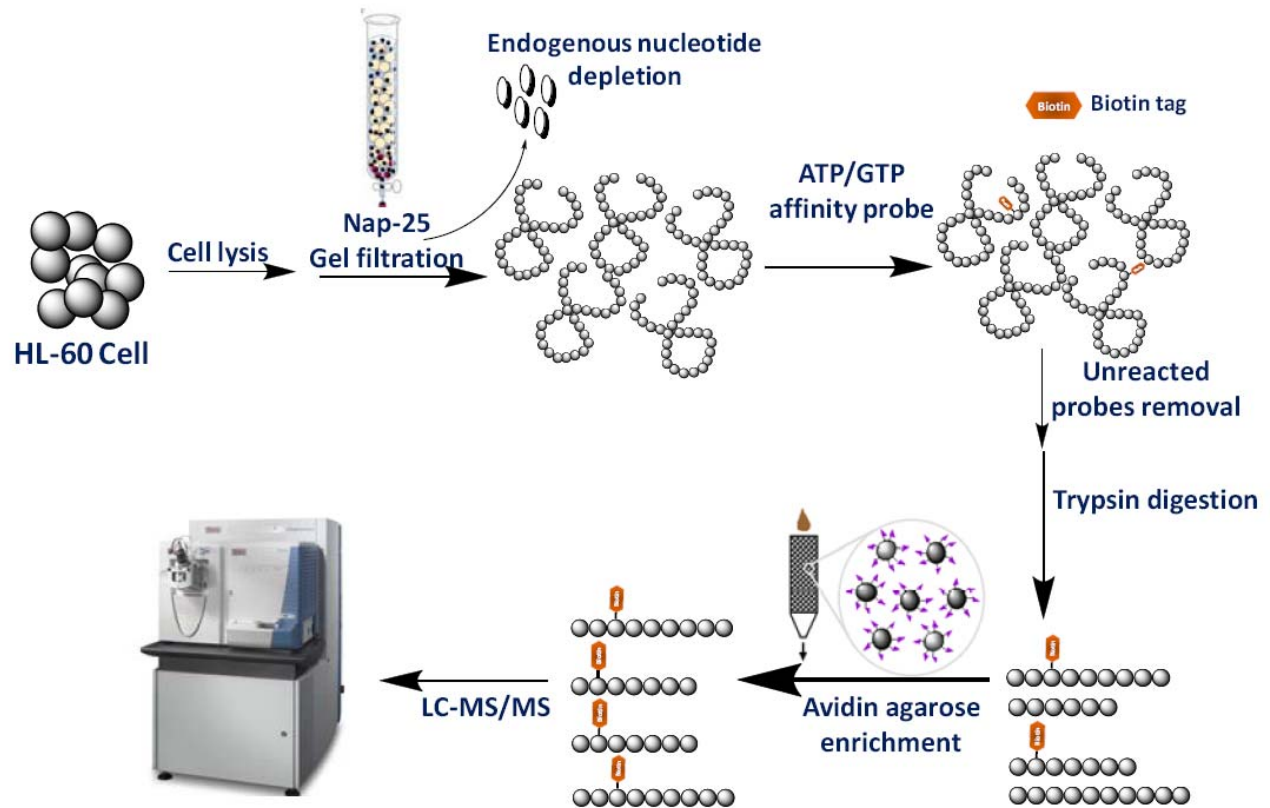
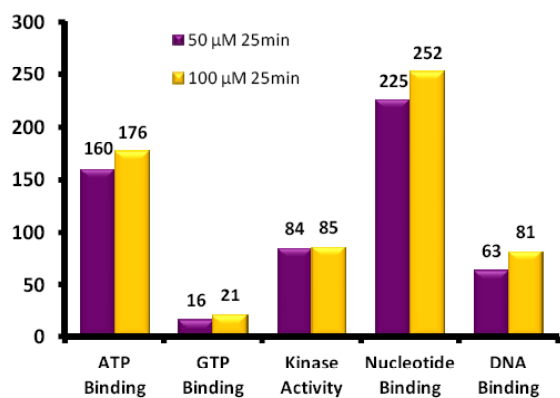
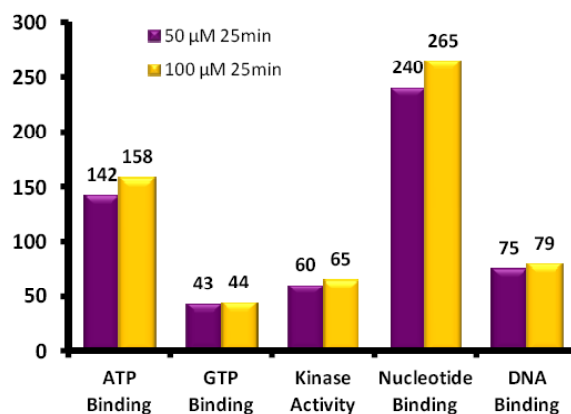


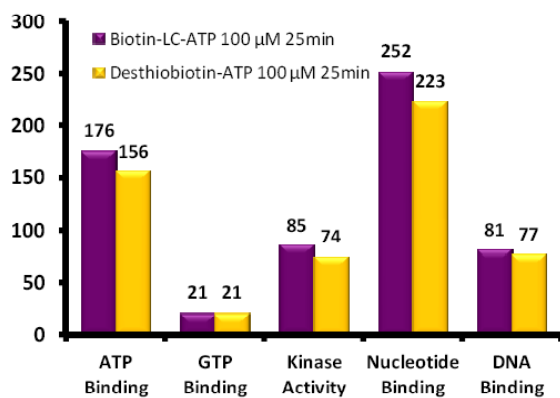
Figure S3. Optimization of the performance of nucleotide-affinity probes for protein detection by varying concentrations of ATP/GTP-affinity probe (A, B) and enrichment moiety (C, D).



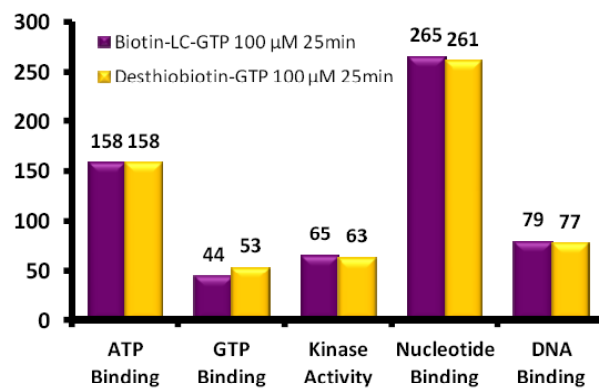
(A) Biotin-LC-ATP probe



(B) Biotin-LC-GTP probe



(C) ATP probe



(D) GTP probe

Figure S4. The Venn diagrams showing all proteins (i.e., identified with probe-labeled peptides, A), known ATP-binding proteins (B), and kinases (C) identified from the reaction of ATP affinity probe with HL-60 cell lysate followed by SDS-PAGE, offline SCX, or online 2D-LC separation.

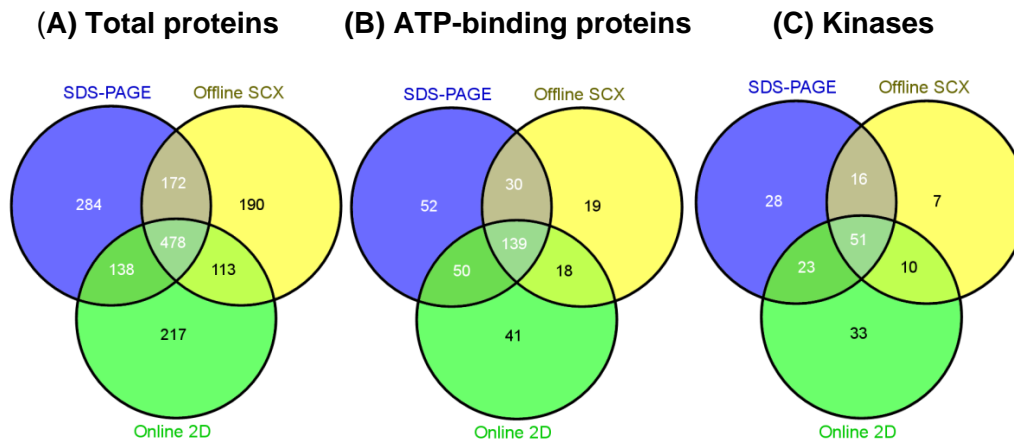
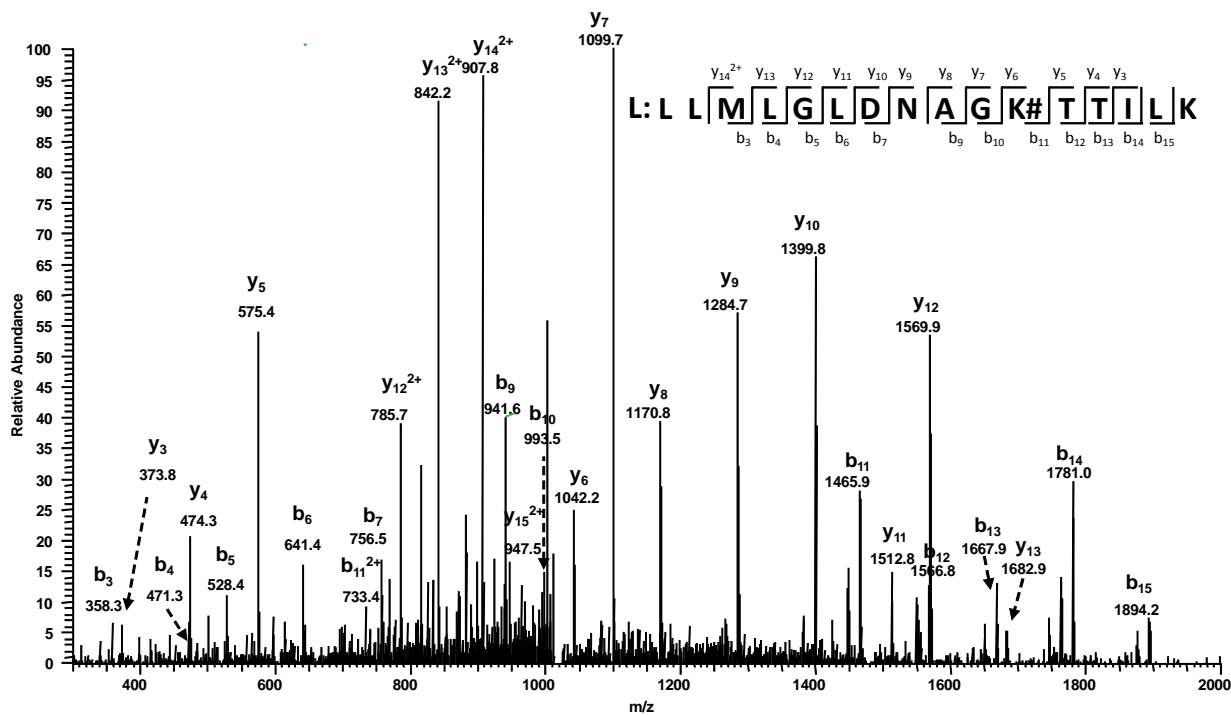
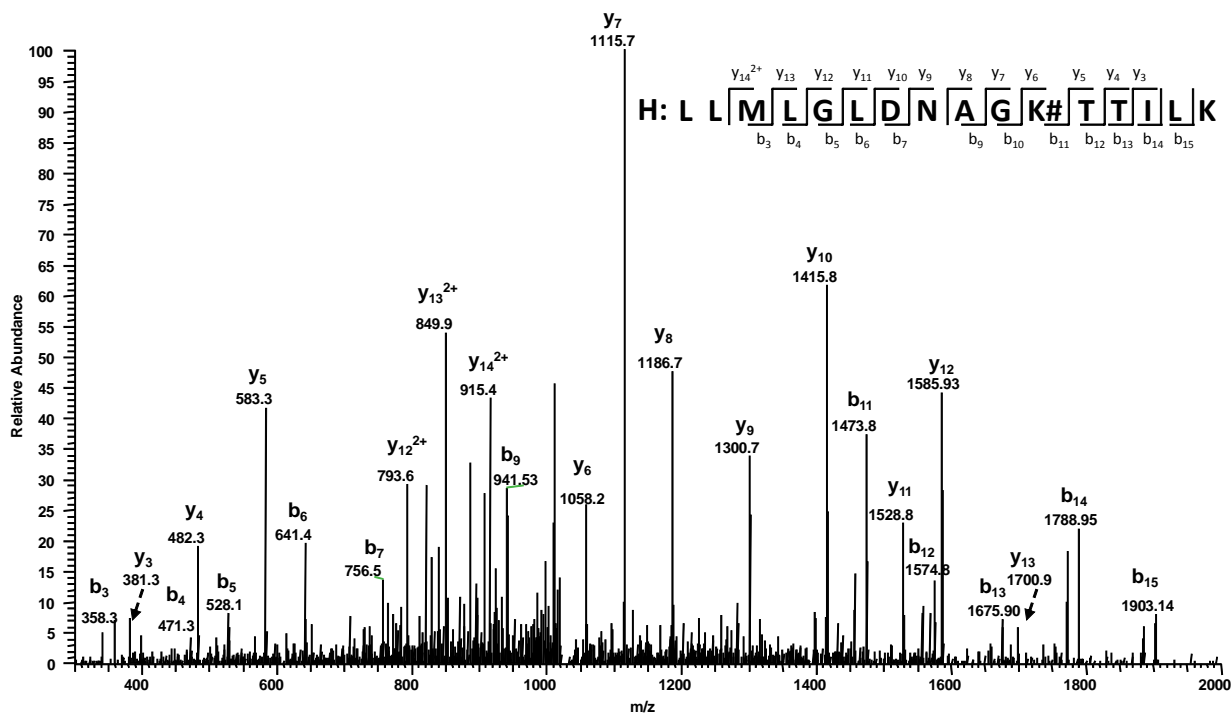


Figure S5. MS/MS of the light- and heavy-labeled LLMLGLDNAGK#TTILK (A, B) from ARL2 and AVLLGPPGAGK#GTQAPR (C, D) from AK2.

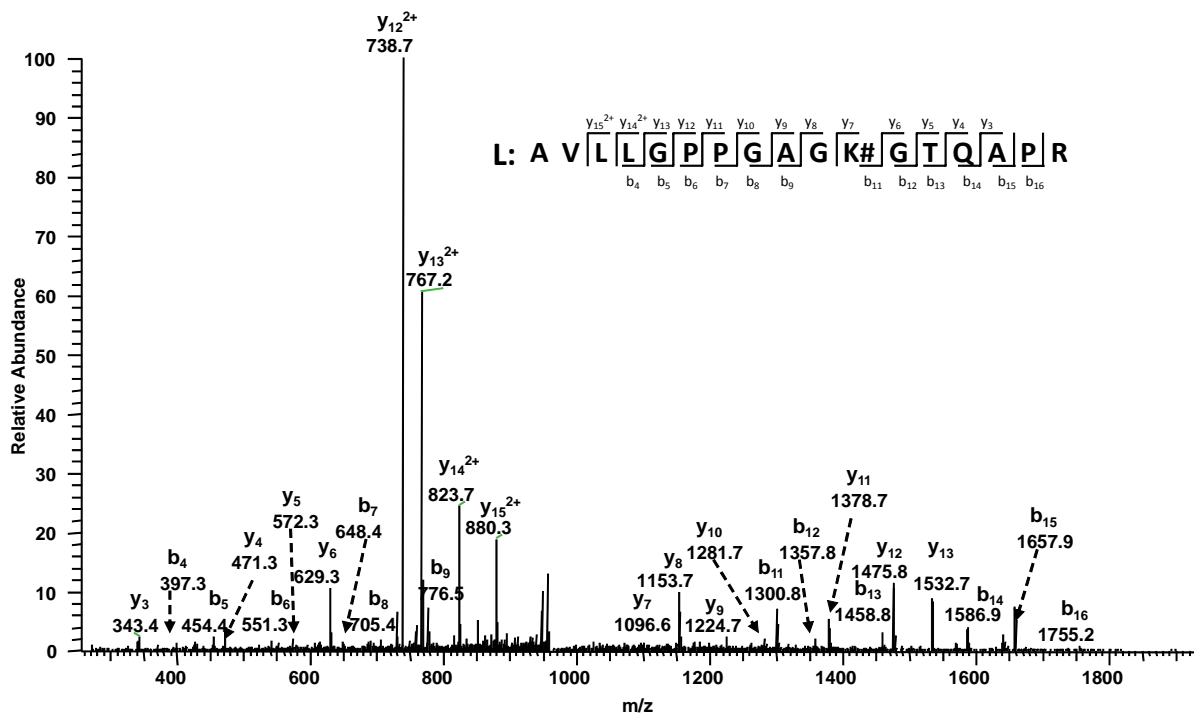
(A)



(B)



(C)



(D)

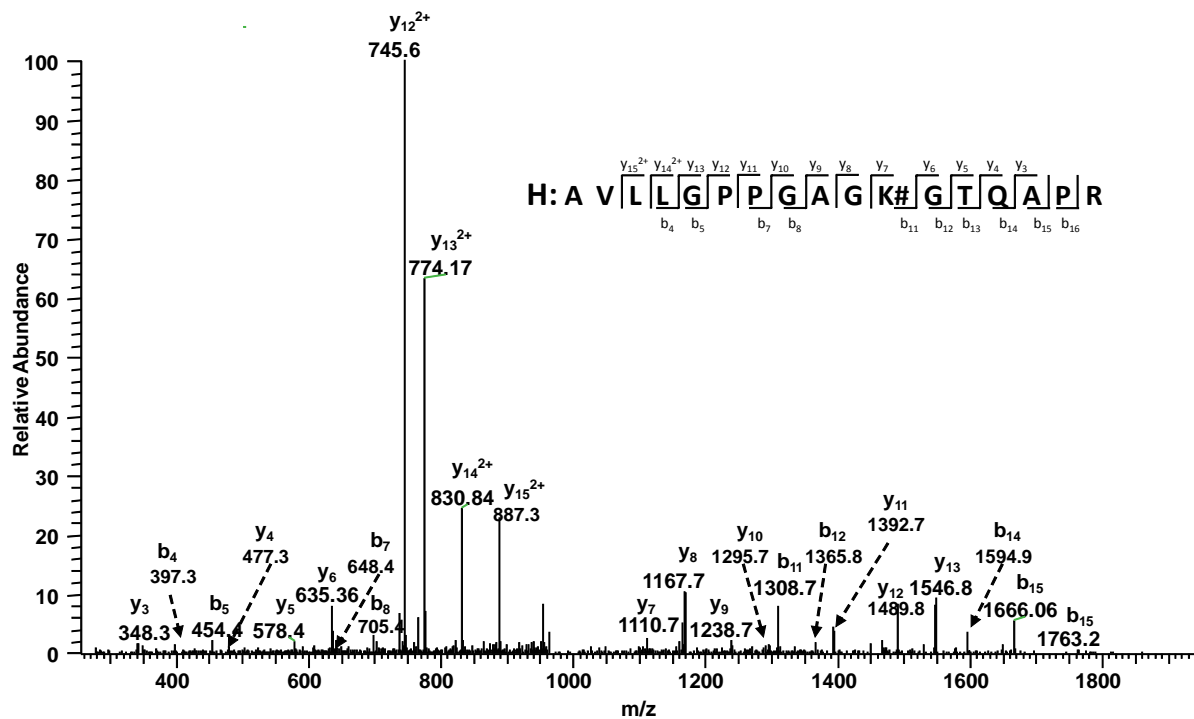


Figure S6. A heatmap showing the relative selectivity of kinases towards ATP/GTP binding based on median $R_{ATP/GTP}$ ratio. Dark blue and white boxes indicate significant ATP-binding preference with high $R_{ATP/GTP}$ ratio and significant GTP-binding preference with small $R_{ATP/GTP}$ ratio, respectively, as indicated by the scale bar above the heatmap.

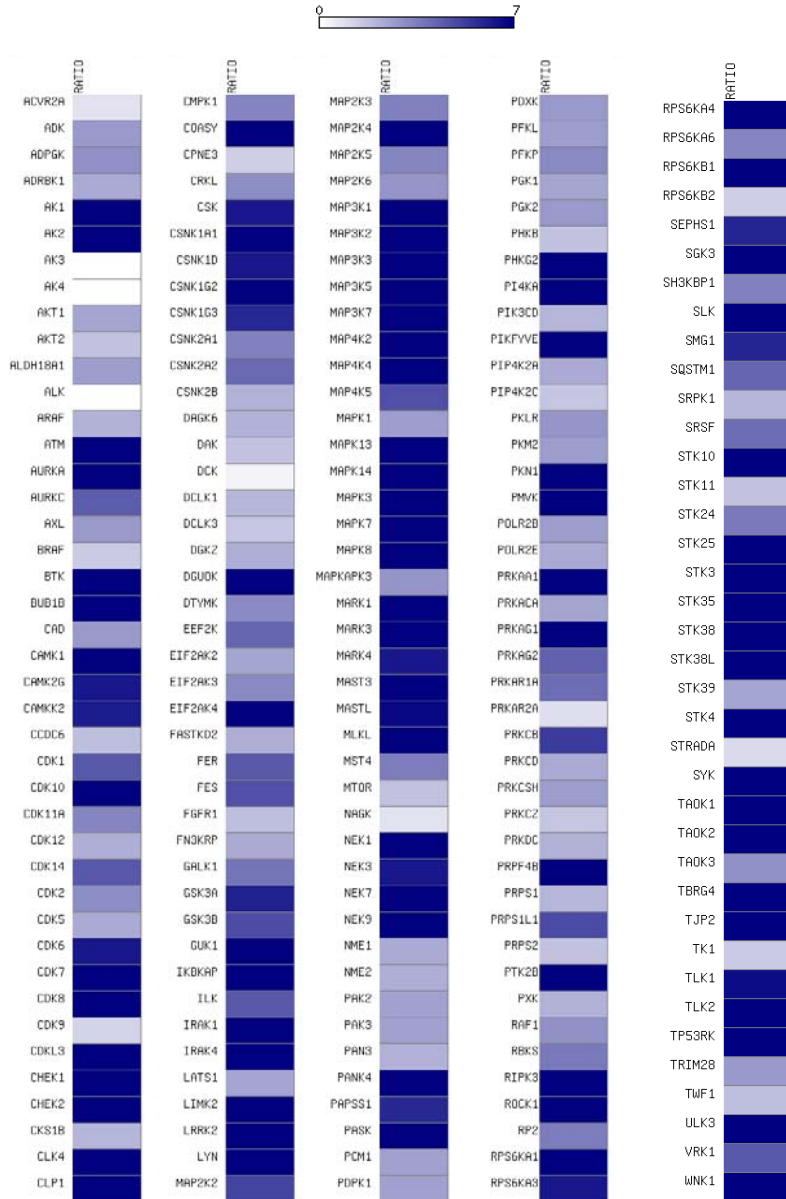


Figure S7. The crystal structures of RPS6KA1 (left) and Lyn (right) bound with ATP.

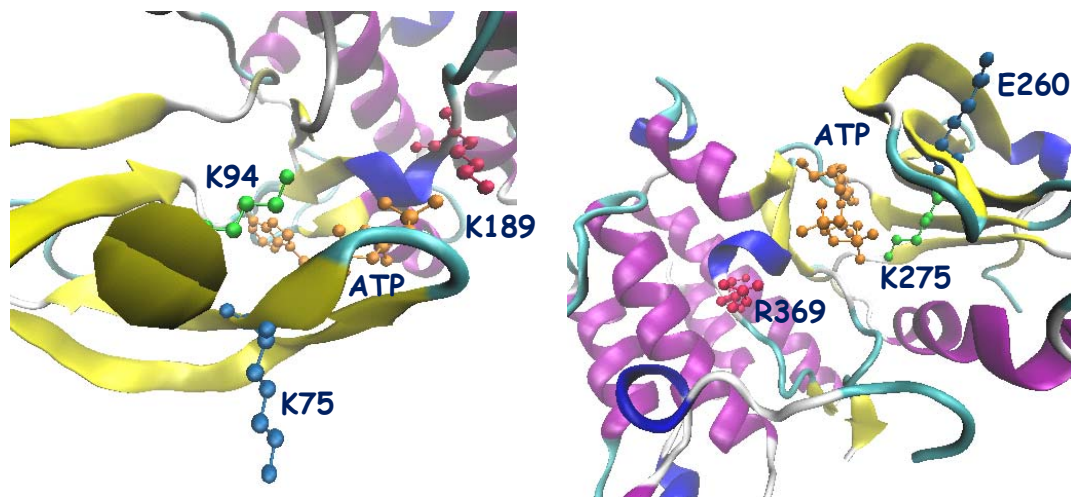


Figure S8. A heatmap showing the relative selectivity of ATP/GTP towards the GxxxxGK motif of GTP-binding proteins.

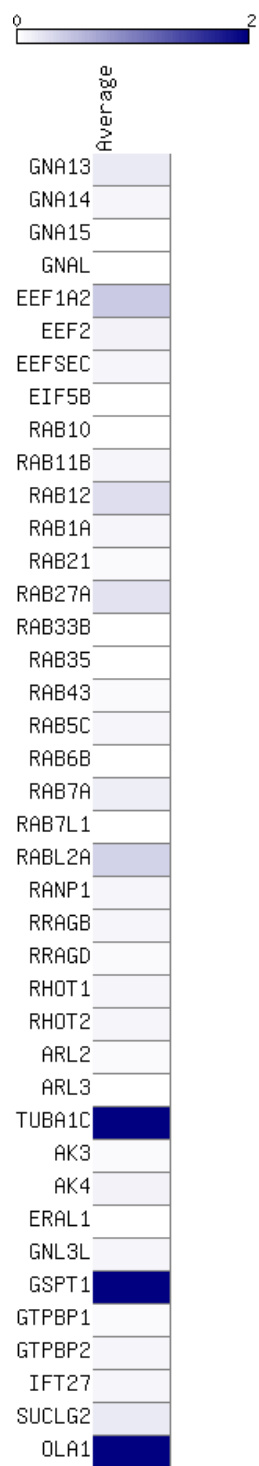


Table S1. Details of Biotin-LC-based and desthiobiotin-based ATP/GTP probe use in each experiment.

Experiments	Probes Used
Large-scale profiling of nucleotide-binding proteins using ATP probe with SDS-PAGE, online and offline 2D-LC separation (section 2)	Desthiobiotin-ATP probe
Large-scale profiling of nucleotide-binding proteins using GTP probe with SDS-PAGE, online and offline 2D-LC separation (section 2)	Biotin-LC-GTP probe
Six run of ATP/GTP competition experiment with 1:1 probe ratio (section 3)	Four runs of Biotin-LC-ATP/GTP probes; Two runs of desthiobiotin-ATP/GTP probes
Four run of ATP/GTP competition experiment with 7:1 probe ratio (section 4, 5)	Desthiobiotin-ATP/GTP probes

Table S2. Quantification results for AK2 in six runs of SILAC-based ATP/GTP (1:1 ratio) competition experiment; Ratio indicates the $R_{ATP/GTP}$ ratio

Protein Name	SEQUENCE	RATIO	DETERMINANT		FILE NAME	SCAN
			FACTOR	XCorr		
Adenylate kinase 2	K.LVSDEMVELIEK#NLETPLCK.N	0.99	0.66	3.25	ATPGTP-1	37797
Adenylate kinase 2	K.LVSDEMVELIEK#NLETPLCK.N	1.13	0.57	3.32	ATPGTP-2	32476
Adenylate kinase 2	R.AVLLGPPGAGK#GTQAPR.L	2.65	0.99	4.94	ATPGTP-1	23939
Adenylate kinase 2	R.AVLLGPPGAGK#GTQAPR.L	2.53	0.99	3.41	ATPGTP-1	23808
Adenylate kinase 2	R.AVLLGPPGAGK#GTQAPR.L	3.04	0.89	2.78	ATPGTP-1	23632
Adenylate kinase 2	R.AVLLGPPGAGK#GTQAPR.L	2.76	1.00	5.03	ATPGTP-2	21322
Adenylate kinase 2	R.AVLLGPPGAGK#GTQAPR.L	2.30	0.99	3.03	ATPGTP-3	27337
Adenylate kinase 2	R.AVLLGPPGAGK#GTQAPR.L	2.29	0.99	5.26	ATPGTP-3	27210
Adenylate kinase 2	R.AVLLGPPGAGK#GTQAPR.L	2.29	0.99	3.97	ATPGTP-3	27023
Adenylate kinase 2	R.AVLLGPPGAGK#GTQAPR.L	2.13	0.99	4.41	GTPATP-1	23364
Adenylate kinase 2	R.AVLLGPPGAGK#GTQAPR.L	2.04	0.98	5.18	GTPATP-2	18985
Adenylate kinase 2	R.AVLLGPPGAGK#GTQAPR.L	2.04	0.98	3.73	GTPATP-2	19105
Adenylate kinase 2	R.AVLLGPPGAGK#GTQAPR.L	2.26	0.99	2.70	GTPATP-3	27822
Adenylate kinase 2	R.AVLLGPPGAGK#GTQAPR.L	2.24	0.99	5.25	GTPATP-3	27803
Adenylate kinase 2	R.AVLLGPPGAGK#GTQAPR.L	2.24	0.99	4.49	GTPATP-3	27597
Adenylate kinase 2	R.AVLLGPPGAGK#GTQAPR@.L	2.53	0.99	2.98	ATPGTP-1	23809
Adenylate kinase 2	R.AVLLGPPGAGK#GTQAPR@.L	2.65	0.99	5.14	ATPGTP-1	23574
Adenylate kinase 2	R.AVLLGPPGAGK#GTQAPR@.L	2.76	0.99	5.10	ATPGTP-2	20711
Adenylate kinase 2	R.AVLLGPPGAGK#GTQAPR@.L	2.61	0.99	3.38	ATPGTP-2	20755
Adenylate kinase 2	R.AVLLGPPGAGK#GTQAPR@.L	2.30	0.99	3.14	ATPGTP-3	27042
Adenylate kinase 2	R.AVLLGPPGAGK#GTQAPR@.L	2.29	0.99	5.11	ATPGTP-3	26836
Adenylate kinase 2	R.AVLLGPPGAGK#GTQAPR@.L	2.04	0.99	3.06	GTPATP-1	23376
Adenylate kinase 2	R.AVLLGPPGAGK#GTQAPR@.L	2.13	0.99	5.25	GTPATP-1	23732
Adenylate kinase 2	R.AVLLGPPGAGK#GTQAPR@.L	1.11	0.86	2.76	GTPATP-2	19059
Adenylate kinase 2	R.AVLLGPPGAGK#GTQAPR@.L	2.08	0.99	4.92	GTPATP-2	19527
Adenylate kinase 2	R.AVLLGPPGAGK#GTQAPR@.L	1.92	0.99	2.99	GTPATP-2	18995
Adenylate kinase 2	R.AVLLGPPGAGK#GTQAPR@.L	2.26	0.99	3.10	GTPATP-3	27675
Adenylate kinase 2	R.AVLLGPPGAGK#GTQAPR@.L	2.24	0.99	5.14	GTPATP-3	27425

Table S3. Identification data for all proteins, ATP-binding proteins, kinases and GTP-binding proteins from ATP affinity probes reacted with cell lysates; identification data for all proteins, ATP-binding proteins and GTP-binding proteins from GTP affinity probes reacted with cell lysates (shown as Excel file in online Supporting Information).

Table S4. A list of quantified protein with medium $R_{ATP/GTP}$ smaller than 1 and average $R_{ATP/GTP}$ ratio of individual probe-labeled peptides in 7:1 ATP/GTP competition experiment, and a list of 14 known ATP-binding proteins with medium $R_{ATP/GTP}$ ratio smaller than 1 in 7:1 ATP/GTP competition experiment (Shown as Excel file in online Supporting Information). The results were based on two sets of forward and two sets of reverse SILAC labeling experiments.

Table S5. A list of quantified protein and the average $R_{ATP/GTP}$ ratio of probe-labeled peptides for known kinases and GTP-binding proteins in 7:1 ATP/GTP competition experiment. Listed also are the $R_{ATP/GTP}$ ratios of peptides with binding motifs from kinases and GTP-binding proteins (Shown as Excel file in online Supporting Information). The results were based on two sets of forward and two sets of reverse SILAC labeling experiments.